Chapter 2

Theory

The work described within this thesis is based upon the classical pair - potential description of the lattice. This is one of the most common computational techniques used in the atomistic simulation of solids and to describe point defects in materials. Their success can be accredited to the fact that they require comparitively less computer time for solving problems, than do their quantum mechanical equivalents.

2.1 Historical Overview Of Computer Simulation

2.1.1 Bulk Simulations

Theoretical studies of solids and surfaces have become increasingly common in the past 30 or so years, due to the availability of progressively cheaper and more powerful computers. This has also been parallelled by improvements in the methodologies [35, 36, 37] and [38].

Initial studies used classical pair potential models to study highly ionic materials such as the alkali [39, 40] and alkaline earth halides, [41, 42]. Presently a number of more complex and technologically relevant materials have been modelled by a variety of techniques: including electronic materials such as High T_C oxides [43, 44], alumino silicates such as zeolites [45, 46] and refractory ceramics such as Alumina [47, 48] to name a few examples. In addition to static studies, there have been a number of classical molecular dynamics studies based on solving Newton's equations of motion. Such studies have been able to shed light on processes such as melting and evaporation [49, 50]. More recently, computer simulations have been used to study the catalytic reactions at surfaces [51] and in zeolite cages [52].

Finally, the recent releases of new more user friendly codes [53] and access to molecular visualisation software [54, **?**] will undoubtedly play an important role in extending modelling studies of complex materials and important reactions.

2.1.2 Surfaces

In comparison to the simulation of bulk materials the theoretical study of surfaces and interfaces is a relatively new field. Seminal studies were carried out by Tasker [55, 56] and Mackrodt [57] on the surfaces of MgO and Al_2O_3 respectively. Indeed, the technique has been so successful that recently it has become possible not only to predict the atomic structure of ionic surfaces [58, 59] but also crystal morphologies; both of ionic [60] and covalent systems [61, 62].

Recently, simulations have been carried beyond merely studies of free surfaces to the modelling of thin films [63, 64], and the development of interfacial models [65]. Such models may eventually lead to models of grain boundary behaviour, which dominate the properties of polycrystalline materials.

Finally, the work of Schluger [66] has shown that it is possible to model the behaviour of an AFM tip on a surface. Consequently this technique has begun to make predictions for the very experimental methods on which the model parameters for the initial simulations were based.

The present review has only given a few examples of the wealth of work employing atomistic techniques. More comprehensive reviews of the techniques and literature can be found in the articles edited by Harker and Grimes [35], [36], and the numerous articles written by Catlow such as [38], [67], and [68].

2.2 Born Model of Ionic Solids

Classical simulation is based upon the description of the lattice in terms of the Born ionic model [69]. The crystal is assumed to be composed of spherical formally charged ions.

Such ionic crystals can be described in terms of the interatomic forces between the ions as a function of their atomic positions (the potential model). Here forces are resolved into a Coulombic contribution and the short range force, such that the lattice energy is given by

$$E_{Total} = \sum \left(\frac{q_1 q_2}{r_{ij}} + E_{short-range} \right) \tag{2.1}$$

where $E_{short-range}$ is the 'short range' energy between the ions i and j. The Coulombic contribution corresponds to the electrostatic interactions between the ions. In the present work formal charges have been assumed, consequently the electrostatic energy is pre-defined, and the quality of the model is dependent on an accurate calculation of short range energy.

2.2.1 The Short Range Potential

The short range force has both repulsive and attractive energy contributions. The repulsive interactions arise from the overlap of the electron clouds which results in an increased nuclear repulsion as the ions are brought closer to each other by bond formation. A second contribution to the repulsive energy arises from the Pauli exclusion principle, due to a change in the confinement of the electron. The attractive contribution occurs through the formation of instantaneous dipoles, these induce similar dipoles in neighbouring ions, which act in a comparable way. When such behaviour correlates across the entire crystal or macromolecule, it results in an overall attractive force. The magnitude of this force is dependent on the 'hardness' or polarisability of the ions and is greater in so called 'soft' ions e.g. large ions such as I^-, which have loosely bound outer electrons.

Mathematically the short range energy can be expressed as a binomial expansion,

$$E_{short-range} = \sum_{ij} S_{ij} + \sum_{ijk} \theta_{ijk} + \sum_{ijkl} T_{ijkl} \ldots\ldots \tag{2.2}$$

where S_{ij} refers to all two body interactions, θ_{ijk} refers to all three body interactions (bond bending), T_{ijkl} refers to torsional interactions and so on. In many ionic solids the two body forces tend to dominate as they have isotropic structures. In addition, many two body potential parameters are derived from emprical fitting (discussed in section 2.3) which effectively incorporate any residual many body contributions into these parameters. Consequently higher order terms are omitted in the present work, and will not be discussed further.

As mentioned above, the Coulombic contribution is a constant in the present work, consequently the success of any simulation study is dependent on the description of the short range energy. The quality of this model is limited by the analytical form chosen to describe the potential and also the numerical values of the variable parameters employed within the given function.

Several analytical funtions may be used to represent the two body interaction. The simplest being the harmonic interaction to represent bonding,

$$S_{ij}(r) = 1/2k(r - r_e)^2 \tag{2.3}$$

where r_e is the equilibrium bond distance. This description is perfectly acceptable for small deviations from the equilibirium distance, which still exhibit harmonic behaviour. However for a more refined description, which is valid at large separations a modified version of this potential is used, a Morse interaction:

$$S_{ij}(r) = D[1 - exp[-\beta(r - r_e)]]^2 \tag{2.4}$$

where D is the dissociation energy of the bond, r_e is the equilibrium bond length and β is a variable parameter determined from spectroscopic data. This analytical form is often used for the modelling of covalent molecules.

Non - bonded interactions are commonly represented by the Lennard - Jones potential,

$$S_{ij}(r) = \frac{A}{r^{12}} - \frac{B}{r^6} \tag{2.5}$$

where A and B are parameters which represent the repulsive and attractive forces respectively. This potential has been used successfully to model liquids [70] and metals [71]. For inorganic solids the most commonly used potentials are the Born -

Mayer and Buckingham interactions. Equation 2.6 is the Born - Mayer interaction which is a repulsive potential and is used to model ‘hard’ cation - anion interactions,

$$S_{ij}(r) = Aexp(-r/\rho) \tag{2.6}$$

for ‘soft’ ion interactions an attractive term is added to this function, to form a Buckingham.

$$S_{ij}(r) = Aexp(-r/\rho) - \frac{C}{r^6} \tag{2.7}$$

the terms A, ρ, and C are three variable parameters. Roughly speaking, these parameter are dependent on the ion size, hardness and dispersive effects respectively. The present work predominantly uses the Buckingham and Born-Mayer analytical forms.

An important point about such analytical forms is that they converge to zero when r = ∞. Hence in computer simulations a cut off is employed to keep the computational time to a realistic duration. Nonetheless, the cut off must not be too small otherwise the function will not be close enough to zero which may affect the lattice energies (Figure 2.1).

2.3 Potential Derivation

As mentioned previously the success of any simulations is dependent not only on the choice of function but also on the values of the parameters. The present section deals with methods for the determination of parameters for Buckingham and Born-Mayer interactions.

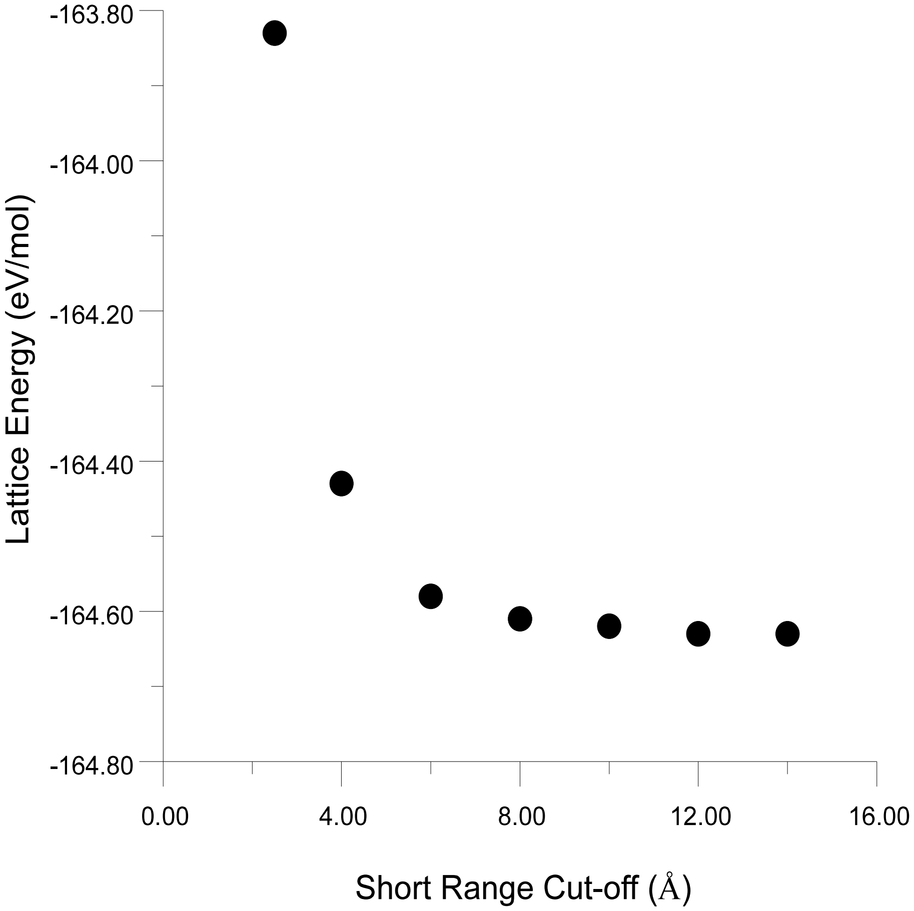

Figure 2.1: The lattice energy as a function the potential cut-off for CeO_2

2.3.1 Empirical Derivation

This commonly used method has the advantage of being a relatively simple way to derive reliable parameters; many of the potentials in the present work have been calculated in this way. The technique involves varying the parameters of the function iteratively, such that they give the best fit to experimental values which are dependent on the potential model such as: the unit cell volume, experimental lattice parameter, phonon dispersion curves, and the dielectric and elastic constants of the system in question. This technique has been automated to a certain extent in the code GULP [53], by the use of a linear least squares fitting routine. The method is summarised in the flow chart, Figure 2.2.

The disadvantage of this method is that it effectively relies on a single point on the potential energy hyper-surface; that corresponding to the equilibrium interionic separation of the system. Hence, it is assumed that the potential parameters will accuratly reproduce the short range force at a distance significantly different from the equilibrium separation, Figure 2.3, at which they were derived

Recently [72], [59], this method has been improved upon, by fitting the potential to several different structures simultaneously. Hence the parameter are defined with respect to several different ionic separations i.e the equilibrium separation of the different structures. Consequently, the potential derived by this method should be significantly more reliable when used in defect calculations and at surfaces where the intrinsic distances may deviate significantly from those in the bulk material.

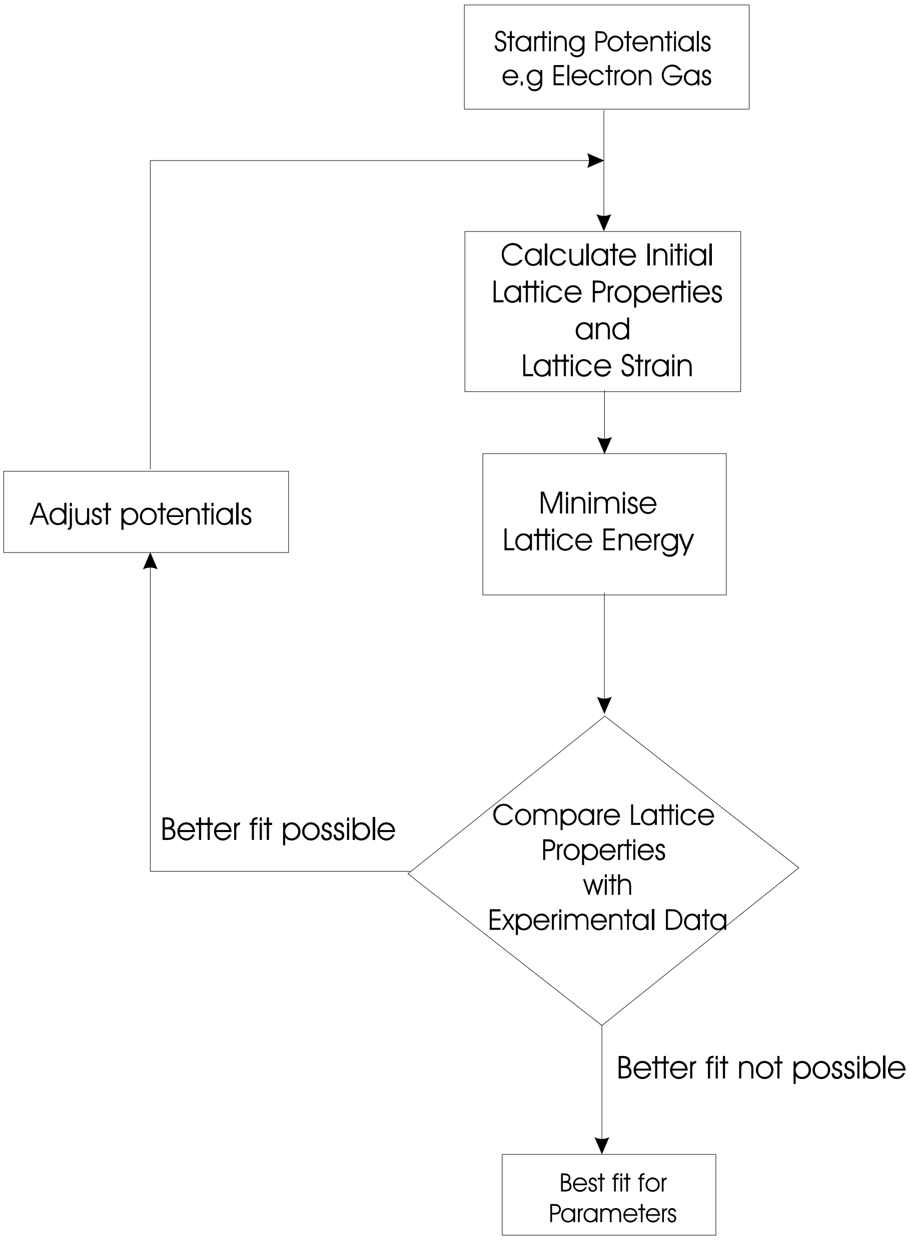

Figure 2.2: Flow chart representation of empirical potential derivation

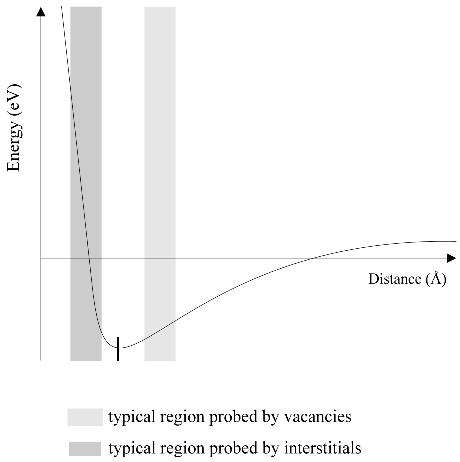

Figure 2.3: Interionic distances

2.3.2 Electron Gas Potentials

This is a method based on quantum mechanical techniques [73, 74] . The interaction between two atoms is calculated assuming that each ion has a spherically symmetric charge distribution whose wavefunction is determined either numerically or analytically. Both methods assume a one electron wavefunction for the ion and express it in terms of a single Slater determinate. Once the ionic charge densities have been calculated the total energy (E_T) of the two interacting ions is written as the sum of seperate energy components.

$$E_T = E_{Elec} + E_{Ke} + E_{Exch} + E_{Corr} + E_{Disp} \tag{2.8}$$

Where, E_{Elec} is the electronic energy contribution, E_{Ke} is the kinetic energy, E_{Exch} the exchange energy, E_{Corr} the correlation energy, and E_{Disp} the dispersive contribution to the total energy. The potential parameters can be derived by fitting an analytical form to the variation of the total energy as a function of distance. What makes this method so computationally efficient is that E_{Ke}, E_{Corr}, and $_{Exch}$ can be expressed as being proportional to specific powers of the electron density [74]. A more detailed discuss about electron gas potentials is given by Harding and Harker in [75].

2.3.3 Empiricised Potentials

It has been shown [11], [76] that a reliable model of the short range forces cannot necessarily be derived if potentials from different sources are combined together. This is found to be especially true when electron gas potentials are mixed with empirically derived potentials. However, electron gas potentials are incredibly useful in cases where no experimental data are available; such as in the modelling of transition states and point defects. Nevertheless, such potentials can be combined by the technique of empiricisation. This entails finding the difference between an appropriate fitted potential and its electron gas equivalent. This difference can then be added to the required electron gas potential. The resulting 'empiricised potential' is more compatable with the fitted potentials. Figure 2.4 shows a graphical representation of this method for the derivation of a Ce^{3+} - O^{2-} potential.

2.3.4 Other Methods

In addition to the techniques used in the present work, several other methods of parameter derivation exist. The most common is the use of quantum mechanical methods to determine the potential energy hypersurface. By determining the interaction energy for a range of ionic separations or molecular configurations, a description of the short range energy can be derived. The parameters of the function (e.g. A, ρ, and C for a Buckingham potential) can then be calculated using a least squares fit to the hypersurface [77], [78]. The advantage of this method is that the potentials are

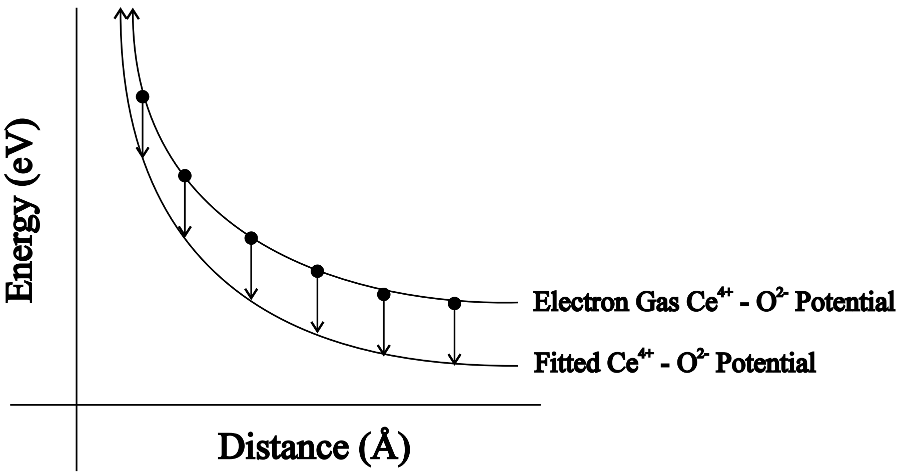

1. Calculate shift, (↧), between Fitted and Electron Gas Potentials

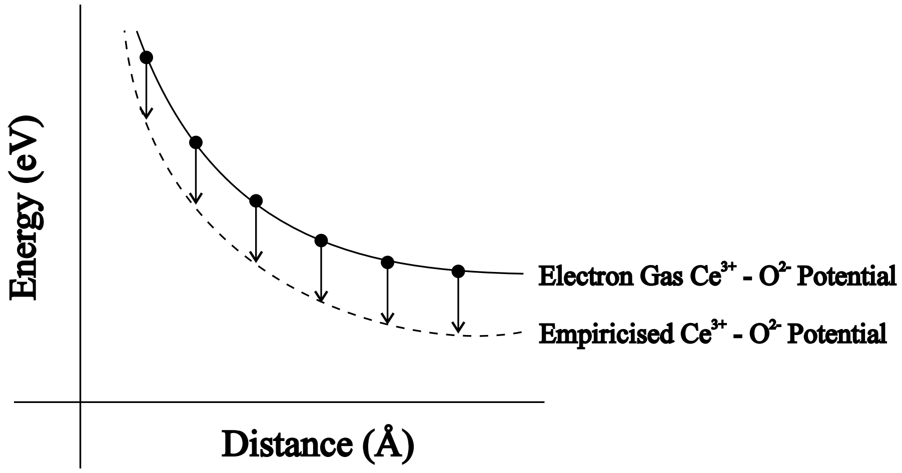

2. Add shift to new Electron Gas Potential to produce `Empiricised' potential

Figure 2.4: Empiricising Potentials

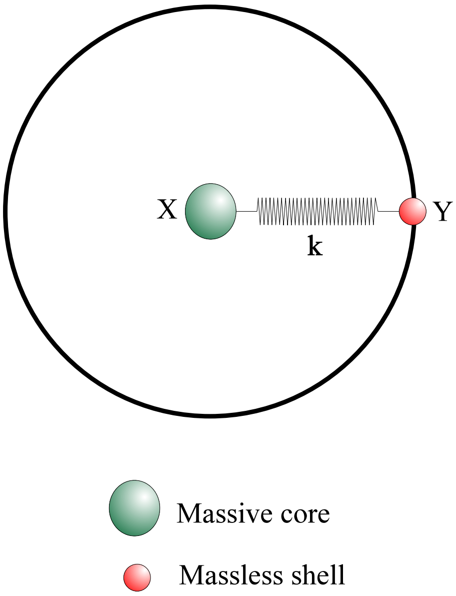

Figure 2.5: The shell model

valid for a range of interatomic separations. However, such methods tend to be very computationally expensive which makes them less attractive at present. No doubt, as computing power increases they will become more common.

2.4 The Shell Model

The parameters we have discussed so far assume the electronic orbitals are fixed and have little effect on the lattice energy. Obviously, this is not a completely accurate picture of a 'real' system. The electron clouds can polarise to a certain extent, the magnitude of which is dependent on the nature of the system being studied.

One of the simplest and most successful methods for taking into account the polarisation of ions within the Born model is the shell model developed by Dick and Overhauser [79]. In this model the ion is treated as consisting of a spherical massless shell, of charge Y, and a core of charge X. The core is bound to the shell by a harmonic spring of force constant, k. The charge state of the ion is equal to X+Y. The polarisation is represented by the displacement of the shell relative to the core (Figure 2.5). The degree of polarisation is dependent on the value of the harmonic spring constant and the shell charge. The free ion polarisabilty is given by the equation,

$$\alpha = 14.993\frac{Y^2}{k} \tag{2.9}$$

where Y is in units of e and k is in evÅ^{-2}.

The shell model is primarily used for the modelling of anions, where polarisation effects can be of significant importance. Nonetheless, the shell model has been sucessfully applied to cations, in particular heavy ions such as U^{4+} [80, 81].

An advantage of the shell model is its ability to couple the short range potentials with the polarisabilities (Figure 2.6). This coupling is achieved by assuming that any interactions between ions only occur via the shells. The physical basis of the model is that the short range interactions are a result of electron cloud interactions. These electron clouds can be polarised by nearby ions. Given this, the shell can be viewed as representing the valence electrons (although this is not completely accurate), hence the short range force must act between the shells.

2.5 Perfect Lattice Simulation

The initial step for any simulation study is the calculation of the lattice energy of the perfect crystal by equation 2.1. Other crystal properties such as the elastic constants

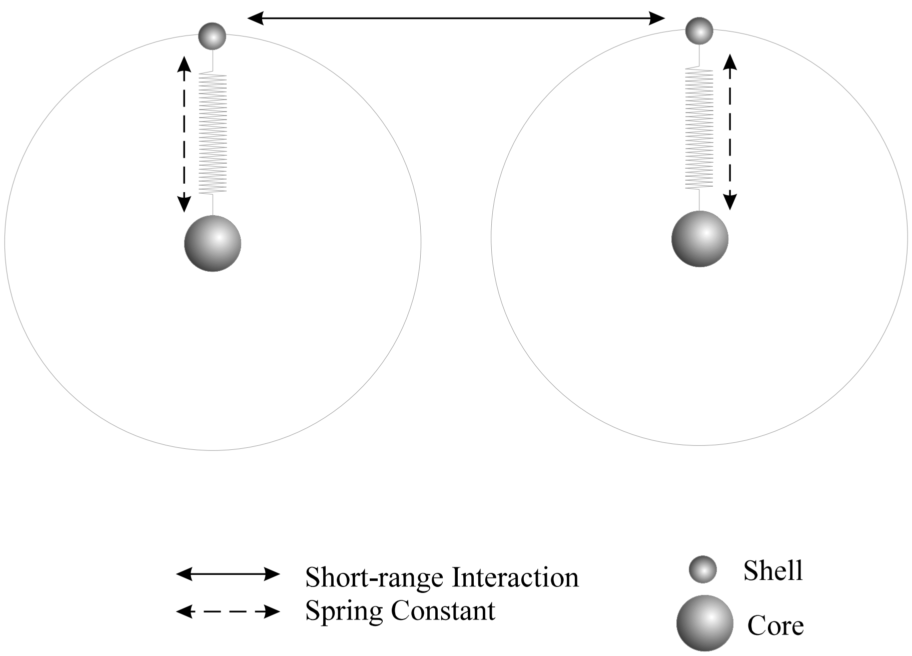

Figure 2.6: The coupling of shell model and the Born ionic model

and dielectric constants and phonon frequencies can be calculated by taking the first and second derivatives of this energy with respect to the atomic coordinates.

2.5.1 The Ewald Summation

The Coulombic part of equation 2.1 is a long range interaction, consequently the convergence of the summation is non-existent when carried out in real space. In addition, the convergence is conditional and dependent on the number of atoms in the summation.

The solution to the problem was provided by Ewald [82], the technique entails resolving the electrostatic term into two parts; one is summed in real space and the other in reciprocal space. The electrostatic potential of an ion can be resolved into two parts,

$$\phi = \phi_1 + \phi_2 \tag{2.10}$$

ϕ_1 is based on a lattice of Gaussian charge distributions situated at each ion site. The sign of this charge distribution is the same as that for the real ion. However, the charge contribution of the ion for which the potential is being calculated must be subtracted. Thus, ϕ_1, can be expressed as,

$$\phi_1 = \phi_L - \phi_i \tag{2.11}$$

ϕ_2 is based on a complete lattice of point charges with an additional Gaussian distribution of opposite charges (Figure 2.7). The reason for the use of a Gaussian charge distribution is that by a suitable choice of the peak width parameter, η, rapid independent convergence of both ϕ_1 and ϕ_2 can be achieved.

ϕ_L, ϕ_i, and ϕ_2 can be related to the charge density, ρ, which in the case of a Guassian distribution is

$$\rho = q_t \left(\frac{\eta}{\pi}\right)^{3/2} exp(-\eta r^2) \tag{2.12}$$

where q_t is the ion charge. ϕ_L can be given by,

$$\phi_L = \frac{4\pi}{V} \sum_{\mathbf{G}} S(\mathbf{G}) \frac{1}{\mathbf{G}^2} exp \frac{\mathbf{G}^2}{-4\eta^2} \tag{2.13}$$

where S($\mathbf{G}$) is,

$$S(\mathbf{G}) = \sum_t q_t exp(-i\mathbf{G} \cdot r_t) \tag{2.14}$$

where $\mathbf{G}$ is the reciprocal lattice vector and V is the unit cell volume. For the reference ion i, the potential is given by the expression,

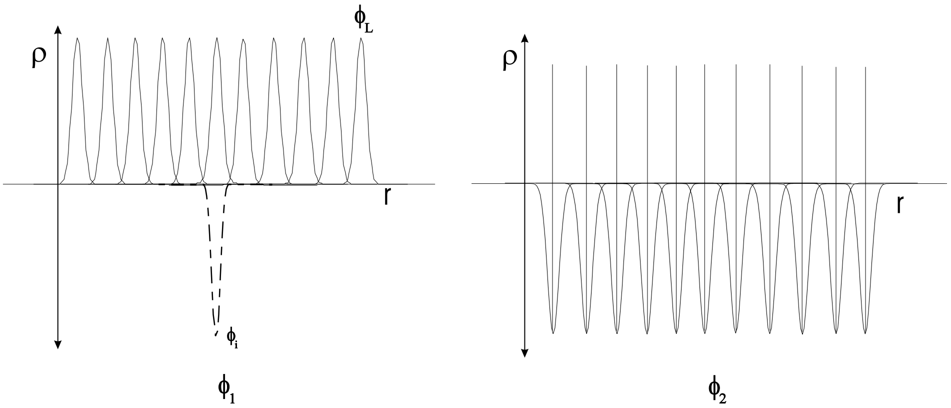

Figure 2.7: The Gaussian charge distribution for ϕ_1 andϕ_2.

$$-\phi_i = -2q_i \left(\frac{\eta}{\pi}\right)^{1/2} \tag{2.15}$$

For ϕ_2,

$$\phi_2 = \sum_l \frac{q_l}{r_l} F(\eta, r_l) \tag{2.16}$$

where F(x) is given by,

$$F(x) = (2\pi^{1/2}) \int_x^\infty exp(-s^2)dt \tag{2.17}$$

The optimum value of η was determined by Catlow and Norgett, [83], to be given by the expression,

$$\eta = \left(\frac{N\pi^3}{V^2}\right)^{1/6} \tag{2.18}$$

where N is the number of species (both ions and shells), and V is the unit cell volume. For a more comprehensive explanation the reader is referred to Kittel [84].

2.5.2 Energy Minimisation Techniques

From the discussion in the previous sections, it is possible to determine the lattice energy of the system. However, to determine equilibrium geometries the potential energy must be minimised with respect to the systems atomic coordinates, i.e. the unit cell vectors and internal parameters. The system can be minimised if the coordinates are adjusted iteratively until the forces on the atoms are zero, i.e.:

$$\frac{\partial U}{\partial \mathbf{r}} = 0 \tag{2.19}$$

where U is the lattice energy and **r** is the coordinate system.

Several minimisation algorithms are available, each having its own particular merit. These include the Conjugate Gradient [85], Steepest descent [85], and the Newton-Raphson methods [86]. The primary factors in determining the choice of minimisers are their computational cost and ability to avoid local minima and transition states (see Figure 2.8) which satisfy the minimisation criteria that equation 2.19 is zero.

The two methods used in the present study are the Conjugate Gradient and the Newton Raphson techniques.

Conjugate Gradient

The value of the position vector **x** at the (n+1)th iteration is related to its nth iteration by,

$$\mathbf{x}_{(n+1)} = \mathbf{x}_n + \alpha_n S_n \tag{2.20}$$

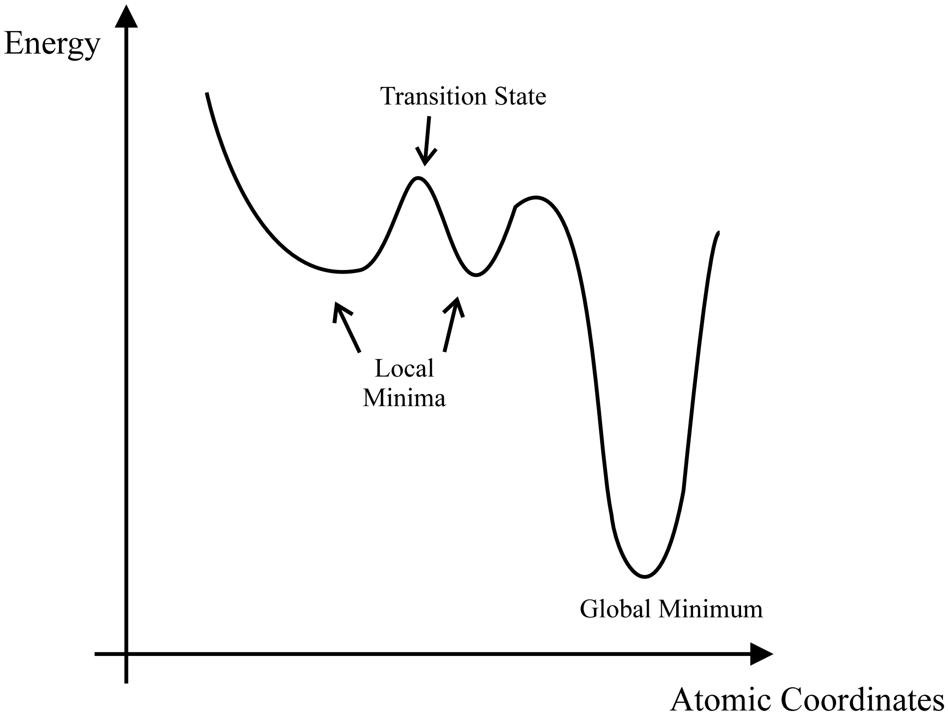

Figure 2.8: A typical example of a potential energy hypersurface

where α is a constant modified at every iteration to improve the efficiency of the algorithm. S is given by the expression

$$\mathbf{S_n} = -\mathbf{g_{i-1}} + \beta_\mathbf{i} \tag{2.21}$$

where, β is,

$$\beta = \frac{\mathbf{g_{i-1}^T . g_{i-1}}}{\mathbf{g_{i-2}^T . g_{i-2}}} \tag{2.22}$$

and $\mathbf{g}_i$ are the first derivatives of the vectors and the 'T' notations indicates the transpose of the vector. This method has a very low computational cost (as only the first derivatives are calculated) and very rapid convergence at large distances from the minimum. However, as it approaches the minimum the method becomes inefficient.

Newton-Raphson

Convergence can be improved by the use of second derivatives in addition to the first. In the Newton-Raphson technique, $\mathbf{x}_{(n+1)}$ is given by,

$$\mathbf{x}_{(n+1)} = \mathbf{x}_n - Hi.\mathbf{g}_i \tag{2.23}$$

where H is the inverse of the second derivative matrix, also known as the Hessian matrix. The second derivative matrix contains the second derivatives of the energy with respect to the ion coordinates. The Hessian matrix is not recalculated at every iteration as it makes the computation prohibitively expensive. Instead it is updated using various algorithms such as the Davidson, Fletcher and Powell method [87]. To avoid too great a degradation in the accuracy of the Hessian, it is recalculated every

10-20 cycles. This approach is particularly good at achieving rapid convergence close to the minimum.

2.5.3 Constant Pressure and Volume Minimisation

The minimisation of the lattice geometry to equilibrium can be either done at a constant volume, or at a constant pressure. Constant volume minimisation, as the name suggests, is where the unit cell volume is kept constant during minimisation. This is achieved by only varying the internal ion positions of the unit cells to remove the ionic strains. The set of lattice coordinates $r^{'}$ are related to the lattice coordinates r by the expression

$$r^{'} = \mathbf{E} \cdot (r + \delta r) \tag{2.24}$$

where $\mathbf{E}$ is a Voigt matrix representation of the indepedent bulk strain components, $\delta\epsilon$. When minimising to constant volume the strain in the ion coordinates is removed,

$$\frac{\partial U}{\partial \delta r} = 0 \equiv g \tag{2.25}$$

Hence it can be shown that the optimum displacement of an ion at point r from equilibrium is

$$\delta r = -\mathbf{W}_{rr}^{-1} \cdot g \tag{2.26}$$

where $\mathbf{W}_{rr}^{-1}$ is the Hessian matrix. If the energy of the system were perfectly harmonic with respect to the strain, equation 2.26 would give the value of r, and hence the lattice energy at the minimum. However in reality this is not the case the equation must be solved by an iterative procedure.

For constant pressure calculations, in addition to the energy being minimised with respect to the ionic coordinates, it is also minimised with respect to the bulk strains acting upon the cell. These bulk strains are defined such that they transfer every vector in the lattice to $r^{'}$, where

$$r^{'} = (\mathbf{E} + \mathbf{I}) \cdot r \tag{2.27}$$

where **I** is known as the identity matrix and **E** is the strain matrix discussed previously. The strains are calculated assuming Hooke's Law, with a constant of proportionality given by the elastic constant tensor. The stress is the first derivative of the lattice energy with respect to the strains, thus the bulk strain, $\delta\epsilon$, is given by

$$\delta\epsilon = \frac{\partial U}{\partial \delta\epsilon} \cdot \mathbf{C}^{-1} \tag{2.28}$$

where C is the elastic constant matrix. More detailed discussion can be found in Catlow and Norgett [83] and [37]

2.6 Defect Lattice Simulation

The properties of many materials are not only dependent on their perfect lattice properties but also on the defects present within them. Often this can be critical, such as in controlling the mechanical strength of a material. Consequently, studies of defects in the lattice are of considerable importance.

Once a valid perfect lattice model has been derived, it can be used to study defects in the lattice. The inclusion of such defects within the lattice is a rigorous test of the potential model. The distortion of the lattice ions caused by the presence of defects will change the interionic distances considerably. Hence the potentials must be robust enough to deal with such changes in the interionic spacing. In an ionic lattice the pertubations caused by a charged defect can be quite large and long range. Consequently, the lattice must undergo further relaxation to reach a new equilibrium geometry.

The defective lattice is treated as consisting of two regions (Figure 2.9) which are considered at different levels of approximation. The inner region (region I) is treated atomistically; the atoms are relaxed explicitly to zero force. The outer region, region II, extends to infinity. The forces arising from the defect are considered to be sufficiently weak that the response of the lattice to the defect can be expressed by the Mott-Littleton approximation [88]. This describes the response of the (cubic) lattice at a distance **r**, from the defect centre in terms of polarisation,

$$\mathbf{P} = \frac{4\pi}{V} \frac{q\mathbf{r}}{|r|^3} \left(1 - \frac{1}{\epsilon_0}\right) \tag{2.29}$$

where **P** is the polarisation of the crystal per unit cell, ϵ_0 is the static dielectric constant, V is the unit cell voloume and q is the defect energy.

The outer region II is further partitioned into region IIa and region IIb. The forces and displacements on the region IIa ions are determined by the Mott - Littleton approximation. The ions are reacting to the displacements of the region I species which gives rise to short and long range interaction energies, which are calculated explicitly. The positions of the ions in region IIb are not altered and their response to a defect (i.e. the energy change) can be calculated directly by the Mott-Littleton approximation.

The partitioning can be explained using the following mathematics. The total

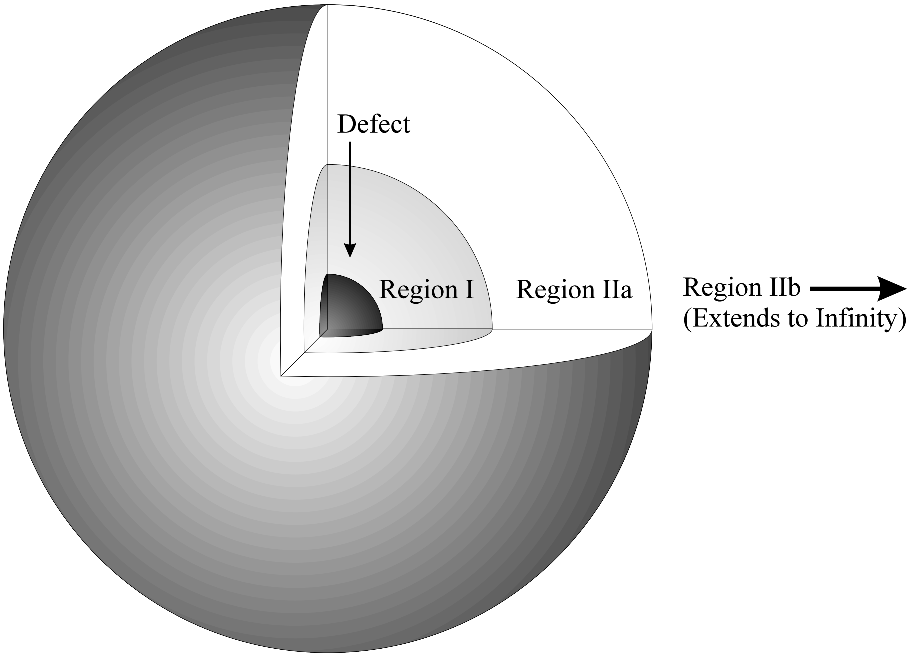

Figure 2.9: The two region methodology

energy of the system can be expressed as a function of the displacement of the ions in region I, **r**, and region II, ζ. The energy is given by the expression

$$E_T = E_1(r) + E_2(r, \zeta) + E_3(\zeta) \tag{2.30}$$

where E_1 is the energy of the region I, E_2 is the interaction energy between region I and region II, and E_3 is the energy change of region II.

$E_3(\zeta)$ cannot be solved exactly as it contains an infinite number of displacements. However, if region I is large enough then the displacements in region II are small enough to be treated harmonically and E_3 can be represented by a quadratic function,

$$E_3(\zeta) = \frac{1}{2}(\zeta.\mathbf{A}.\zeta) \tag{2.31}$$

where **A** is the force constant matrix. Substitution of this expression into equation

2.30 and then differentiating it with respect to ζ, results in

$$\frac{\partial E_T}{\partial \zeta} = \frac{\partial E_2(r,\zeta)}{\partial \zeta} + \mathbf{A}.\zeta \tag{2.32}$$

At equilibrium $\partial E_T/\partial\zeta = 0$ and $\zeta = \zeta_e$, thus

$$\frac{\partial E_2(r,\zeta)}{\partial \zeta} = -\mathbf{A}.\zeta \tag{2.33}$$

Thus equation 2.30 can be expressed as,

$$E_T = E_1(r) + E_2(r,\zeta) - \frac{\zeta}{2}\left(\frac{\partial E_2(r,\zeta)}{\partial \zeta}\right)_{r,\zeta=\zeta_e} \tag{2.34}$$

Hence the dependence of E_T on E_3 is removed and the energy can be expressed as the interaction within region I and the interaction between region I and region II. Thus the calculation scheme for the defect energy is

(i) The energy of region I ions is minimised and **r** is calculated using $\partial E/\partial r_{\zeta=constant} = 0$.

(ii) The Mott-Littleton calculation is perfomed to derive the displacements of region IIa.

(iii) The energy of E_1 is explicitly summed.

(iv) E_2 and its first derivatives are calculated explicitly for the ions in region IIa.

(v) The Mott-Littleton approximation is used to calculate the displacements in region IIb assuming a continuum response to the net defect charge.

The techniques mentioned in this and the previous section have been incorporated in the CASCADE [89] and GULP [53] codes.

2.7 Surface Simulation

Many of the techniques used in the simulation of bulk systems can be readily applied to surface studies given a few minor modifications. Primarily, whilst bulk calculations employ a crystal lattice that extends to infinity in three dimensions, surfaces by their nature are finite in one direction. The required surface is thus constructed from a block repeated periodically in two dimensions (Figure 2.10). The repeat block is divided into two regions, analogous to that discussed in the previous section on bulk defect simulations. Region I contains the free surface, within it all the atoms are relaxed explicitly to their energy minimum. Region II marks the beginning of the bulk and is there to model the effect of the bulk ions on the region I atoms. However, unlike bulk simulations region II does not extend to infinity. Consequently, region II must be large enough to ensure that its finite size does not have an energy consequence on the ions at the bottom of region I. The optimum size is determined by progressively increasing the region II size (for a given region I size) until there is no change in the total energy of region I. In addition, region I must be large enough to ensure that the ions at the bottom of the region do not move significantly during relaxation.

Another modification in the modelling of surfaces is the summation of the electrostatic terms. The three dimensional Ewald sum must be modified to account for the discontinuity in one direction. This was first achieved by Parry [90], [91] for two dimensional slabs. A more comprehensive treatment was derived by Heyes *et al* [92]. Mathematically the two dimensional Ewald sum can be expressed as,

$$U_{ab}^{Ewald} = U_{ab}^{Reciprocal} + U_{ab}^{Real} \tag{2.35}$$

Heyes showed that

$$
\begin{aligned}
U_{ab}^{Reciprocal} &= \frac{\pi}{A}\Bigg\{ -2z_{ab}erfc(Gz_{ab}) - 2\frac{exp(Gz_{ab}^2)}{\pi^{1/2}G} \\
&+ \sum_{\mathbf{k}\neq 0} \frac{exp(i\mathbf{k}.r_{ab})}{|\mathbf{k}|}\Bigg[exp(|\mathbf{k}|z_{ab})erfc\left(\frac{|\mathbf{k}|}{2G} + Gz_{ab}\right) \\
&+ exp(-|\mathbf{k}|z_{ab})erfc\left(\frac{|\mathbf{k}|}{2G} - Gz_{ab}\right)\Bigg]\Bigg\} \qquad (2.36)
\end{aligned}
$$

and

$$U_{ab}^{Real} = \sum_{\mathbf{l}} \frac{erfc(G|r_{ab} + \mathbf{l}|)}{|r_{ab} + \mathbf{l}|} \qquad (2.37)$$

where z_{ab} is the vertical separation between ions a and b. A is the surface area of the simulation cell and **k** and **l** are the two dimensional reciprocal lattice vectors. G is a Gaussian weighting factor and determines how the sum is divided between real and reciprocal space (analogous to η for the three dimesional Ewald summation) and is given by the expression [93],

$$G = \left(\frac{\pi}{A}\right)^{1/2} \qquad (2.38)$$

Such methods have been encoded in surface codes such as MIDAS [94] and the code used in the present work, MARVIN [95].

2.8 Molecular Dynamics

So far, the techniques discussed do not include temperature effects and assume that lattice vibrations behave harmonically. This is valid for small displacements from the equilibrium position. Consequently, within the static model the temperature of the lattice is that of the experimental data used as a basis for fitting the interatomic

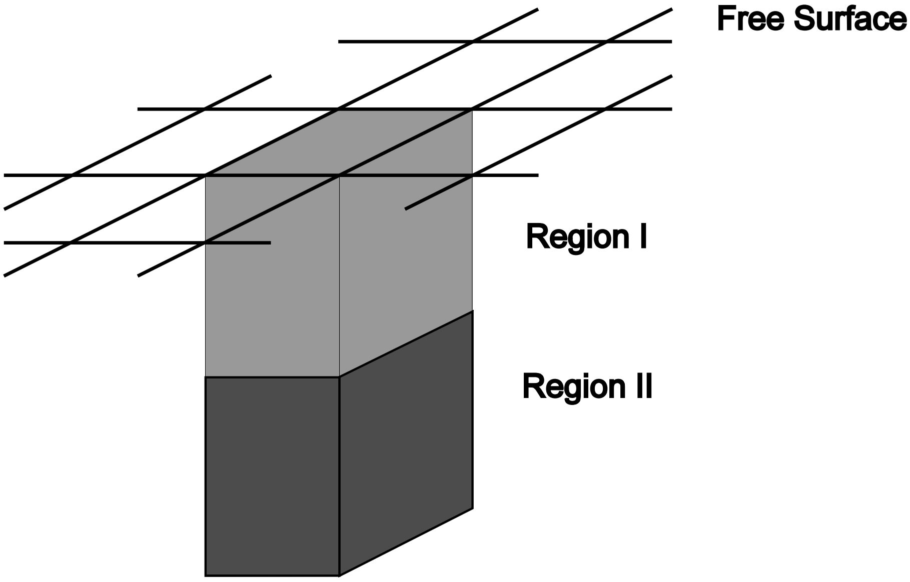

Figure 2.10: Surface simulation methodology

potentials. Such an assumption is adequate when simulating room temperature phenomena or comparing with experimental results carried out at room temperatures. However, at higher temperatures the quasi-harmonic approximation will progressively become less valid and the thermal vibrations of the lattice must be accounted for more explicitly.

Classical molecular dynamics, as the name implies, models the dynamic behaviour of the ions within the lattice. This is achieved by solving the Newtonian equations of motion for the individual ions [96], [97]. The forces acting between the ions can be derived from the pair potentials, by taking the first derivative of the energy. Once the forces on each of the individual ions are known, the acceleration of each species can be calculated using Newton's second law of motion;

$$F = ma \tag{2.39}$$

If the initial velocity and the position are known, then the velocity and position at time (t+δt) can be predicted using

$$v_{(t+\delta t)} = v_t + a\delta t \tag{2.40}$$

and

$$\mathbf{r}_{(t+\delta t)} = v_t\delta t + \frac{1}{2}a(\delta t)^2 + \mathbf{r}_t \tag{2.41}$$

provided that the acceleration is a constant. Under such circumstances the new predicted velocities must not violate the law of conservation of momentum. Thus,

$$\sum_i mv_{i(t+\delta t)} = \sum_i mv_{i(t)} \tag{2.42}$$

The above equations rest on the assumption that the acceleration is a constant. However, this is not the case since the forces between the ions are a function of the ion positions. Consequently, the change in the forces (and hence the acceleration) as a function of δt must be accounted for in the simulations. Several algorithms are available to do this, the method used in the present work is a predictor - corrector algorithm [98], [99]. The position and velocity are predicted using equations similar to 2.40 and 2.41. The acceleration is calculated using the expression

$$a^P_{(t+\delta t)} = a_{(t)} + b_t\delta t \tag{2.43}$$

where b is the third derivative of the position with respect to time. The superscript P indicates this is the predicted acceleration. When the atoms are moved to their predicted positions, the acceleration is recalculated from equation 2.39. The difference between the predicted value of the acceleration and the ‘correct’ acceleration can be expressed as,

$$\Delta a_{(t+\delta t)} = a^{C}_{(t+\delta t)} - a^{P}_{(t+\delta t)} \tag{2.44}$$

This error can be added to the predicted values of position and velocity to correct them, thus,

$$r^{C}_{(t+\delta t)} = r^{P}_{(t+\delta t)} + c_0 \Delta a_{(t+\delta t)} \tag{2.45}$$

$$v^{C}_{(t+\delta t)} = v^{P}_{(t+\delta t)} + c_1 \Delta a_{(t+\delta t)} \tag{2.46}$$

$$a^{C}_{(t+\delta t)} = a^{P}_{(t+\delta t)} + c_2 \Delta a_{(t+\delta t)} \tag{2.47}$$

where c_0, c_1, and c_2 are coefficients that are chosen to give optimum stability.

The size of the time step, δt, must be chosen such that it is not so large as to lead large differences between the predicted and corrected values of positon etc. However, it must not be so small so as to make the calculation require are unrealistically large amount of computer time. Generally, δt is treated as being approximately $1\text{x}10^{-15}$.

The assigning of the initial parameters (velocity, position, and acceleration) is generally done by assigning them randomly using a Gaussian or Boltzmann like distribution. Alternatively, it is possible to use a recursive algorithm. This derives the initial accelerations for very small time step from the initial atomic positions and the interatomic potentials. By applying this recursively until all the atomic derivatives of position are consistent, the atoms will only move from their initial positions to an extent appropriate to the forces resulting from the other ions in the system.

The overall procedure can be listed as;

(i) Assign initial values of velocity, acceleration and position etc using either a random distribution or an algorithm such as the above.

(ii) Predict the position, velocities, acceleration etc at time t+δt using the current values.

(iii) Evaluate the forces and thus the acceleration for the new positions.

(iv) Correct the predicted values using the new accelerations.

(v) Calculate any quantities of interest such as the energy, root mean square displacement, etc.

(vi) Return to step (ii)

The effect of increasing the temperature can be included by the fact that as the energy of a system is increased the velocities of the atoms also increase, thus,

$$T = \frac{2 < \frac{1}{2}mv^2 >}{(3n-6)k_B} \tag{2.48}$$

where k_B is Boltzmann's constant and n is the number of atoms in the system.

More detailed discussion of molecular dynamics methodolgies can be found in Allen and Tildesley [70] and the references within it. The code used in the present study, PENICILLIN, [50] was written at the Royal Instituion by A. Dornford-Smith and further modified by V. Bulatov at Imperial College.

2.9 Summary

This chapter reviews the literature on the computer simulation of surfaces and solids. In addition we have discussed briefly the Born ionic model, the shell model and the methods used to exploit these basic descriptions of ion - ion interaction through computational modelling.